Available online at www.sciencedirect.com

ScienceDirect

www.elsevier.com/locate/jes

JES JOURNAL OF ENVIRONMENTAL SCIENCES

www.jesc.ac.cn

The effect of extracellular polymeric substances (EPS) of iron-oxidizing bacteria (*Ochrobactrum* EEELCW01) on mineral transformation and arsenic (As) fate

Chuan Wu[1,2], *Yueru Chen*[1], *Ziyan Qian*[1], *Hongren Chen*[1], *Waichin Li*[2], *Qihou Li*[3,*], *Shengguo Xue*[1,*]

[1] *School of Metallurgy and Environment, Central South University, Changsha 410083, China*
[2] *Department of Science and Environmental Studies, The Education University of Hong Kong, Hong Kong 999077, China*
[3] *Ministry of Scientific Research, Central South University, Changsha 410083, China*

ARTICLE INFO

Article history:
Received 27 July 2022
Revised 30 September 2022
Accepted 5 October 2022
Available online 17 October 2022

Keywords:
Iron-oxidizing bacteria
Extracellular polymeric substances (EPS)
Arsenic (As)
Biomineralization
Mineral phases transformation

ABSTRACT

Extracellular polymeric substances (EPS) are an important medium for communication and material exchange between iron-oxidizing bacteria and the external environment and could induce the iron (oxyhydr) oxides production which reduced arsenic (As) availability. The main component of EPS secreted by iron-oxidizing bacteria (*Ochrobactrum* EEELCW01) was composed of polysaccharides (150.76-165.33 mg/g DW) followed by considerably smaller amounts of proteins (12.98–16.12 mg/g DW). Low concentrations of As (100 or 500 μmol/L) promoted the amount of EPS secretion. FTIR results showed that EPS was composed of polysaccharides, proteins, and a miniscule amount of nucleic acids. The functional groups including -COOH, -OH, -NH, -C=O, and -C-O played an important role in the adsorption of As. XPS results showed that As was bound to EPS in the form of As^{3+}. With increasing As concentration, the proportion of As^{3+} adsorbed on EPS increased. Ferrihydrite with a weak crystalline state was only produced in the system at 6 hr during the mineralization process of *Ochrobactrum* sp. At day 8, the minerals were composed of goethite, galena, and siderite. With the increasing mineralization time, the main mineral phases were transformed from weakly crystalline hydrous iron ore into higher crystallinity siderite ($FeCO_3$) or goethite (α-FeOOH), and the specific surface area and active sites of minerals were reduced. It can be seen from the distribution of As elements that As is preferentially adsorbed on the edges of iron minerals. This study is potential to understand the biomineralization mechanism of iron-oxidizing bacteria and As remediation in the environment.

* Corresponding authors.
E-mails: liqihou@csu.edu.cn (Q. Li), sgxue70@hotmail.com (S. Xue).

https://doi.org/10.1016/j.jes.2022.10.004
1001-0742/

Introduction

Arsenic (As) is a toxic metal that exists naturally in the environment. In the process of ore mining, smelting, pesticide use and other human activities, As is exposed and released, resulting in the pollution of soils, groundwaters, and farmland, thereby affecting human health (Peng et al., 2021). Soil contamination by As in China was as high as 2.7%, which is among the highest levels seen in Asia (Liu et al., 2020). Excessive accumulation of As in the human body interferes with cell metabolism regulation, affects cell respiration and oxidation, and leads to pathological changes (Ngo et al., 2021). Especially, inorganic As has higher toxicity than organic forms, and according to data for common human diseases, the International Agency for Research on Cancer (IARC) listed inorganic As as the first carcinogen (Zhang et al., 2017). Moreover, the toxicity of arsenite (As(III)) is greater than that of arsenate (As(V)) (Khan et al., 2021). At present, the removal of As from various environments is processed using ion exchange, phytoremediation, adsorption, chemical precipitation, electric, and electrocoagulation methods (Alka et al., 2020). However, traditional physical and chemical technologies include high processing costs and can cause secondary pollution. In contrast, microbial technology has the advantages of low cost and environmental friendliness, with many microorganisms having As tolerance ability found in present studies (Pan et al., 2012).

Iron minerals have been shown to serve as efficient adsorbents in removing heavy metal pollutants from the environment due to their special chemical and structural characteristics, such as second-line ferrite ($Fe_5HO_8 \cdot 4H_2O$), goethite (α-FeOOH), haematite (α-Fe_2O_3), siderite (α-$FeCO_3$), and schwertmannite ($Fe_8O_8(OH)_6SO_4$) (Lu et al., 2014; Kappler and Straub, 2005). Iron-oxidizing bacteria can promote the aggregation of Fe(II), increase the oxidation rate of Fe(II), and promote the formation of iron (oxyhydr) oxides in the environment. Bioderived iron oxides have a larger specific surface area, finer particles, and higher binding energy than chemically generated iron oxides, so they are expected to be more effective adsorbents for As pollution treatment (Kappler and Straub, 2005; Iwahori et al., 2014). The Fe minerals produced by iron-oxidizing bacteria have strong adsorption to As, which can effectively reduce the toxicity of As and hinder its migration (Razzak, 2021). Katsoyiannis and Zouboulis (2004) inoculated iron-oxidizing bacteria into a fixed-bed upflowed filtration device and found that the iron-oxidizing bacteria *Gallionella ferruginea* and *Leptothrix ochracea* generated stem-like or sheath-like iron oxides. The bacteria and their products accumulated in the device, within the filtration column, and As in the water was removed by adsorption. At the same time, bacteria also participated in the catalytic oxidation of As(III), increasing the overall As removal rate to 95%. Xiu et al. (2015) used microaerobic *Pseudomonas* sp. strain GE-1 to induce the oxidation of Fe(II), and As was fixed on hydrous iron ore by adsorption or coprecipitation, accompanied by the redox transformation of As(III) and As(V).

In addition to the generated iron minerals, the extracellular polymeric substances (EPS) produced by iron-oxidizing bacteria also have an adsorption effect on arsenic. EPS are viscous secretions of microbial cells that are distributed in the intracellular layer and tightly bound to the cell surface (Adav and Lee, 2008). Proteins and polysaccharides are the chemical components of EPS and the EPS matrix contains abundant anionic groups. These groups interact with heavy metal ions, endowing bacteria with good adsorption properties. Zhang et al. (2020) demonstrated that the existence of EPS could effectively promote As surface adsorption and limit its intracellular uptake. Liu et al. (2020) also showed EPS was the key factor that influenced As. So, EPS alleviated As toxicity to bacterium and increased As adsorption (Naveed, 2020). In addition, the effect of EPS on As adsorption is also reflected in the mineralization of iron-oxidizing bacteria. EPS produced by bacterial cell surface substances or cell metabolism have an especially important regulatory significance on the formation of iron minerals and have a certain regulatory effect on the nucleation sites of the initial crystal growth of iron minerals (Chan et al., 2009). Alginate polysaccharides in mineralized filaments produced on the surface of neutral iron-oxidizing bacteria *Leptothrix* sp. and *Gallionella ferruginea* have been shown to play a role in inducing the formation and localization of FeOOH (Chan et al., 2004). The effects of organic matter such as dextran, chitosan, and gelatine on microbial mineralization could regulate the nucleation, crystal structure, and growth orientation of iron minerals (Sun and Huang, 2006). Different types of iron-oxidizing bacteria and organic substances, such as polysaccharides and proteins, participate in the regulation of the formation of various iron minerals with different mineral phases and crystal structures and, thus, have an important impact on the fate of heavy metals in the environment (Miot et al., 2009; Zeng et al., 2022). Clapa et al. (2019) found that EPS produced by iron-oxidizing bacteria was of great significance in the immobilization of As, and the minerals produced were submerged in the EPS matrix.

The above studies confirmed that EPS produced by iron-oxidizing bacteria and its biomineralization products have advantages in As removal. Although studies reported that the presence of As may have promoted microorganisms to produce increased amounts of EPS, As is highly toxic to organisms (Saba et al., 2019; Huang et al., 2019). It is obscure whether particular Fe(II)-oxidizing bacteria have a detoxification mechanism to allow them to function normally in the presence of highly toxic As (Chen et al., 2020). Moreover, especially the effects of As on EPS formation and related biomineralization remains unclear. In our previous study, we isolated an iron-oxidizing bacteria *Ochrobactrum* EEELCW01, and proved its biomineralization and As remediation ability in paddy field (Luo et al., 2020; Wu et al, 2022). However, the effect of EPS of this iron-oxidizing bacteria *Ochrobactrum* sp. on mineral transformation and As fate has not been studied. The present study investigated: first, the growth curve of *Ochrobactrum* sp., which has a degree of resistance to As, was observed by culturing it at different As concentrations; then, the EPS composition of cultured bacteria was analysed to determine the effect of As concentration on its formation; third, the effect of As on EPS formation as well as the biomineralization process was further verified.

1. Materials and methods

1.1. Strain and culture medium

In this study, the nitrate-dependent iron-oxidizing bacterium *Ochrobactrum* EEELCW01 was isolated from a typical As-contaminated paddy soil in Changsha City, Hunan Province. Based on morphological and 16S rRNA gene sequence analysis, the bacterium was identified as Bacillus paleus, and its accession numbers in the NCBI GenBank are CP047598 and CP047599. When the strain was activated, *Ochrobactrum* EEELCW01 was removed from the refrigerator at -80°C and inoculated in sterilized LB medium under sterile conditions. The strain was activated for 24 hr in a shaker at 28°C and 180 r/min.

1.2. Determination of bacterial growth curve

The activated iron-oxidizing bacteria were inoculated into liquid LB medium containing 0, 100, 500 and 1,000 μmol/L $NaAsO_2$, and the inoculation amount was 5% (*V*/*V*). Medium without As solution was used as the blank control in observing the experimental effect of As on growth. The strain was cultured at 28°C and 180 r/min for 7 days, and the suspension in the medium was sampled at each interval of approximately 2–8 hr. To precipitate the insoluble medium, the suspension was kept for 15–20 min, and the optical density (OD_{600}) was measured to create the growth curve for this strain of iron-oxidizing bacteria.

1.3. Extraction and purification of EPS

EPS was extracted by the alcohol precipitation method. Compared with other physical and chemical extraction methods, the most important feature of the alcohol precipitation method is that it can largely retain the chemical composition and functional groups present in the EPS (Zhou et al., 2020), which is conducive to the subsequent analysis of active groups and other parameters (Yuan et al., 2011).

A total of 2.5 mL of activated iron-oxidizing bacterial solution was inoculated in 250 mL of liquid LB medium containing 0, 100, 500, and 1,000 μmol/L $NaAsO_2$ and cultured at 28°C and 180 r/min for approximately 72 hr until the stable growth of bacteria was ascertained. Bacterial culture medium cultured to the stable phase was loaded into a 50 mL centrifuge tube and centrifuged at 4°C and 5,000 r/min for 15 min to remove bacterial cell precipitate and collect the supernatant. Then, the collected supernatant was centrifuged at 4°C and 12,000 r/min for 30 min in a high-speed refrigerated centrifuge to remove all cell residues. Finally, the collected supernatant was mixed evenly with anhydrous ethanol at a ratio of 1:3. The samples were then stored in a refrigerator at 4°C for 48 hr. The precipitate in the clarification solution was collected by freezing centrifugation, and the collected precipitate contained the crude extract of EPS from iron-oxidizing bacteria.

The crude EPS extract was filtered through a 0.22 μm water filter membrane to remove a small number of residual bacteria. The filtered extract was placed in a pre-treated dialysis bag (MWCO = 3,500 Da), sealed with a dialysis clamp, and placed in a beaker filled with ultrapure water for dialysis. The ultrapure water was replaced every 2–3 hr until the conductivity of the solution in the beaker was less than 20 μS/cm. Finally, the solution in the dialysis bag was transferred into a centrifuge tube for freeze drying to obtain the purified EPS sample, which was sealed and stored in a dryer for further use.

1.4. Iron-oxidizing bacteria mediated biomineralization

150 ml of modified MWMM (modified Wolfe's minimal medium) was prepared: 0.14 g/L KH_2PO_4, 0.2 g/L NaCl, 0.3 g/L NH_4Cl, 0.5 g/L $MgSO_4{\cdot}7H_2O$, 0.1 g/L $CaCl_2{\cdot}2H_2O$, 1 mL/L vitamin solution, and 1 mL/L trace element solution.In addition, 5 mmol/L $FeCl_2{\cdot}4H_2O$ and 10 mmol/L $NaNO_3$ were added to provide Fe(II) and nitrogen sources (nitrate-dependent) for iron-oxidizing bacteria. $NaAsO_2$ was used to adjust the concentration of As(III) in the medium to 500 μmol/L, and the pH was adjusted to 6.8–7.2. The above medium was placed in a 150 mL schering bottle and then autoclaved for sterilization at 121°C for 20 min. When the culture medium was cooled to normal temperature, 24 mmol/L sterilized bicarbonate buffer was added to the culture medium, and N_2 was continuously injected into the culture medium of the schering bottle for approximately 30 min to fully remove O_2.

Activated bacterial liquid (2.5 mL) was inoculated into 250 mL of liquid LB medium and cultured for 24 hr to logarithmic growth phase under the same conditions. The resulting expanded medium was centrifuged at 4°C and 5,000 r/min to collect the cells and rinsed with neutral sterile water at pH 7.0 three times to prepare a resting cell suspension. The prepared 4% (*V*/*V*) cell suspension was inoculated into the above medium and cultured in the dark at 30°C for 7 days in an anaerobic workstation. Mineral precipitate was collected by centrifugation at 4°C and 12,000 r/min.

1.5. Chemical analysis

Determination of polysaccharide content was conducted using anthrone colorimetric method (Liu et al. 2013; DuBois et al., 1956). A 10 mg purified EPS sample was dissolved in 10 mL ultrapure water to yield a 1 g/L EPS solution. Then, 4.0 mL anthrone reagent was added. The samples were heated in a boiling water bath for 10 min, removed quickly and cooled in an ice water bath until room temperature. The absorbance was measured at 625 nm.

Determination of protein content was conducted using the Bradford assay (Bradford, 1976). A 10 mg purified EPS sample was dissolved in 10 mL ultrapure water to yield a 1 g/L EPS solution. An aliquot of 5.0 mL Coomassie brilliant blue G250 reagent was added and allowed to stand for 3–5 min after full mixing. The absorbance was measured at 595 nm.

The sugar content was determined using high-performance anion exchange chromatography (Lee, 1990). Approximately 5 mg of each sample was placed in an ampoule bottle, and 2 mol/L TFA (10 mL) was added and hydrolysed at 120°C for 3 hr. The acid hydrolysis solution was transferred to a tube and dried under a stream of nitrogen; then 5 mL of water was added with vortex mixing. Finally, 100 μL of this solution was diluted to a volume of 1 mL, centrifuged at 12,000 r/min for 5 min, and the supernatant was analysed using IC analysis. Chromatographic conditions: the chromatographic

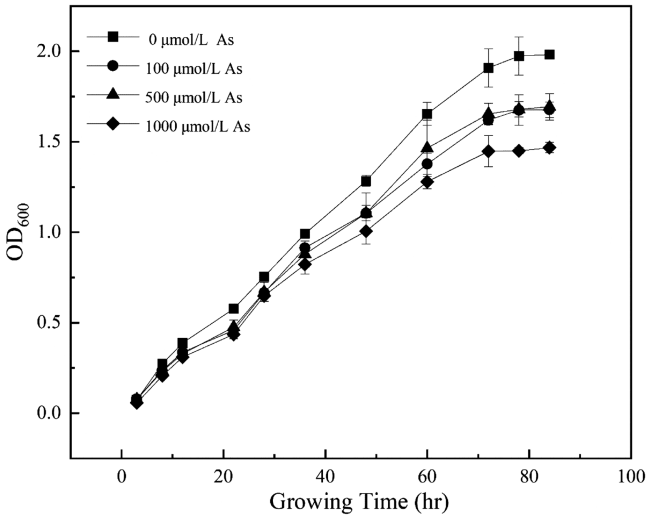

Fig. 1 – Growth curve of iron-oxidizing bacteria at different arsenic concentrations (0, 100, 500 and 1,000 μmol/L $NaAsO_2$).

column was DionexCarbopacTMPA20 (3*150); the mobile phases were A: H_2O, B: 250 mmol/L NaOH, C: 50 mmol/L NaOH and 500 mmol/L NaOAC; the flow rate was 0.3 mL/min; the injection volume was 5 μL; and the column temperature was 30°C.

The effect of As concentration on iron-oxidizing bacteria-EPS functional groups was assessed using Fourier Infrared Spectroscopy.

1.6. *Statistical Analysis*

Data were processed with EXCEL 2017 and IBM SPSS 26.0 and expressed as the mean ± SD of three replicates. ORIGIN2019 was used for data fitting and image processing. Peak fitting of XPS data using Avantage 5.9. FTIR data were analysed by OMNIC.

2. Results and discussion

2.1. *Growth curve of iron-oxidizing bacteria*

Under increasing As concentrations, the growth activity of iron-oxidizing bacteria decreased to various degrees (**Fig. 1**). In the control, without As, the growth rate of iron-oxidizing bacteria was the fastest, reaching a stable growth phase at approximately 72 hr after inoculation with an OD_{600} value of 1.98. In the media containing 100 μmol/L and 500 μmol/L As, the growth rate of iron-oxidizing bacteria was consistent with but slightly lower than the growth rate in the control medium without As, and reached the stable growth stage at approximately 72 hr after inoculation. The OD_{600} values were 1.68 and 1.69, respectively, which were 15.2% lower than that of the control.

Single factor analysis of variance was performed on the OD_{600} values of iron-oxidizing bacteria at different As concentrations after 84 hr of culture. The results showed that the OD_{600} values of iron-oxidizing bacteria at 100 and 500 μmol/L As concentrations were significantly lower than those of the control group, indicating that the low concentration of As solution had an inhibitory effect on the growth and metabolism of iron-oxidizing bacteria, but there was no significant difference between the 100 and 500 μmol/L As treatments, indicating that the iron-oxidizing bacteria had the ability to resist arsenic poisoning within a range of As concentrations. In 1000 μmol/L As-containing culture medium, the growth activity of iron-oxidizing bacteria reached the lowest, and the stable OD_{600} value was 1.47, which was 25.8% lower than that of the control group, indicating that under 1000 μmol/L As culture, iron-oxidizing bacteria were more strongly affected by As, and their growth and metabolism were more significantly inhibited. Compared with the 100 μmol/L and 500 μmol/L treatments, there were significant differences (Tukey, $P < 0.05$). However, in this study, three concentrations of As did not have a strong inhibitory effect on *Ochrobactrum* sp. MYb15 (LD50).

Two reasons may explain why this iron-oxidizing bacteria shows "resistance" to arsenic. On one hand, microbial resistance to As is genetically determined by ars operons. Chen et al. (2020) summarized the arsenic tolerance genes of eight representative Fe(II)-oxidizing bacteria, and represented their As tolerance mechanism. Through genetic testing, Xue et al. (2022) found that several As(III) oxidation genes (aoxA, aoxB, aoxS and arsH) abundance increased with iron-oxidizing bacteria (*Ochrobactrum* EEELCW01). On the other hand, a series of published studies have shown that EPS secreted by bacteria can enhance their resistance to stress caused by toxicity or environmental variability and, thereby, protect cells from high metal concentrations, toxic organic matter, reactive oxygen species, nanoparticles, and other toxic substances (Zhou, 2020). Therefore, we speculated that the detoxification mechanism of arsenic showed in the experiment was related to the EPS secreted by the strain, and further studies were conducted on its EPS.

2.2. *Output and composition of EPS*

The polysaccharide content (150.76–165.33 mg/g DW) in the EPS of the iron-oxidizing bacterium was much higher than the protein content (12.98–16.12 mg/g DW) (**Fig. 2**). Thus, the EPS of iron-oxidizing bacteria was primarily composed of polysaccharides, which is consistent with the study of EPS components of *Thiobacillus ferrooxidans* by Gehrke and Thierry (1998). On the other hand, this result may be due to the high extraction efficiency of polysaccharides by the alcohol precipitation method and the influence of glucose in the medium.

From changes in EPS component content under growth at different concentrations of As, the polysaccharide content reached the highest level at 100 μmol/L As culture, while the protein content reached the highest level at 500 μmol/L As culture. When the As concentration was 1,000 μmol/L, the content of polysaccharides and proteins in the EPS both reached the minimum level. This indicated that under the conditions of 100 and 500 μmol/L As culture, As promoted the secretion of EPS from iron-oxidizing bacteria, and the polysaccharide and protein content in EPS increased. Studies have shown that *Sinorhizobium melilo*, a Cu^{2+}-tolerant bacterium, can regulate its metabolism and secrete more protein complexes with Cu^{2+}

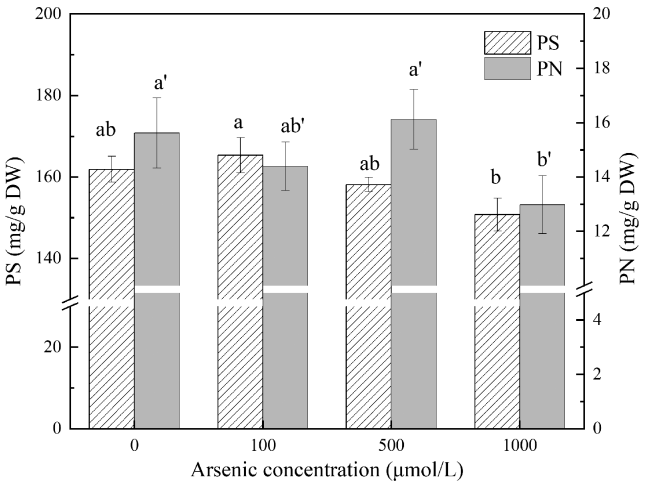

Fig. 2 – Polysaccharide and protein contents in extracellular polymeric substances (EPS) of *Ochrobactrum* sp. cultured at different arsenic concentrations.
Notes: PS: Polysaccharides; PN: Proteins. The same indicator with the same letter means that the difference between groups is not significant ($P>0.05$), and with different letters means that there is a significant difference between groups ($P<0.05$). The same applies below.

in a long-term Cu^{2+} exposure environment to achieve detoxification in the cellular environment (Hou et al., 2013). In addition, studies have shown that extracellular polysaccharides secreted by cyanobacteria and other microorganisms can isolate the organisms from the effects of As^{3+}, Zn^{2+}, Cu^{2+}, Cd^{2+}, Hg^{2+}, and other heavy metal ions, and the removal efficiency can be as high as 90% (Li et al., 2016; Bhunia et al., 2018).

Extracellular polysaccharides were the main component of the extracellular polymer of *Ochrobactrum* sp. MYb15, and many studies have proven that polysaccharide components play a vital role in biosorption and biomineralization. Kang et al. (2017) found that in addition to the significant role in biofilm formation and surface adsorption, reducing sugars in extracellular polysaccharides had a certain redox capacity, but there was no more convincing evidence that it had such an effect on arsenic transformation. Therefore, a more detailed characterization of the molecular structure of EPS is essential for understanding its active ingredients and key components. The exopolysaccharides of iron-oxidizing bacteria were composed of 9 monosaccharides, and the content from high to low was galactosamine hydrochloride (GalN), glucuronic acid (GlcA), glucosamine hydrochloride (GlcN), galactose (Gal), mannose (Man), glucose (Glc), galacturonic acid (GalUA), xylose (Xyl), and arabinose (Ara). **Fig. 3** showed that the absolute content and content percentage of the predominant monosaccharides was: galactosamine hydrochloride > glucuronic acid > glucosamine hydrochloride > lactose > mannose, and these accounted for more than 90% of the total extracellular polysaccharide. The content of each monosaccharide changed according to the various concentrations of As present in the culture conditions. At a low As concentration the monosaccharide content was greater, while at an As concentration of 1000 μmol/L, the monosaccharide content decreased, which was consistent with the change total polysaccharides. Except for glucosamine hydrochloride, other polysaccharides had a maximum amount at an As concentration of 500 μmol/L, and this was predominated by the content of glucuronic acid, glucose, xylose, and arabinose, which were significantly higher at this As concentration than that in other treatment groups ($P < 0.05$).

2.3. *Effect of arsenic concentration on EPS*

The strong, broad-spectrum peak in the range of 3,417.40–3,423.28 cm^{-1} was the stretching vibration of the associated O-H groups in the carbohydrate, and the peak at 2,921.16–2,925.04 cm^{-1} showed the antisymmetric stretching vibration of $-CH_2$ groups on saturated carbon atoms (Govarthanana et al., 2019). The peak at 1,647.37–1,649.00 cm^{-1} indicated the stretching vibration of C=O on amide I bands of typical proteins, and the peak at 1,565.77–1,567.04 cm^{-1} was the superposition of bending vibration of -NH and stretching vibration of -CN on amide II bands (Omoike and Chorover, 2004; Cao, 2013). The peak at 1,414.00–1,418.91 cm^{-1} was the characteristic absorption peak of COO-, which was caused by the stretching vibration of the C-O bond in the carboxyl groups. In addition, the stretching vibration peaks of C-O-C/C-O on polysaccharides appeared at 1,249.31–1,253.05 cm^{-1} and 1,065.47–1,067.03 cm^{-1} (Zhang et al., 2014). Bands in the fingerprint region below 1,000 cm^{-1} may indicate the presence of phosphorus-containing groups, which could be due to the presence of a small amount of nucleic acid groups in EPS (Liu et al., 2020).

In **Fig. 4**, the FTIR absorption peak of EPS after As adsorption changed both in position and intensity compared with that before adsorption. The characteristic peak of -OH shifted from 3,417.40 cm^{-1} to 3,423.28 cm^{-1}, and the peak intensity was significantly enhanced indicating that the content of -OH in the EPS increased after As adsorption (Naveed et al., 2020). Therefore, we speculated that the shift of the -OH group peak is related to the adsorption of As. The carbonyl and amide groups representing the characteristic peaks of proteins had slight redshifts at 1,649.00 cm^{-1} and 1,565.77 cm^{-1}, respectively. The infrared spectrum was a vibration spectrum and the required energy was usually exceptionally low. Moving to a low wave number showed that the energy required for vibration was lower, which indicated that the group was more unstable. This implied that the combination of As with C=O and -NH/-CN on proteins caused the decomposition of protein structure, which was consistent with the previous result in which As led to the weakening of protein content (Cao, 2013). The characteristic C-O-C/C-O peaks of polysaccharides shifted from 1,249.31 cm^{-1} and 1,065.47 cm^{-1} to 1,253.05 cm^{-1} and 1,065.47–1,067.03 cm^{-1} after As adsorption, respectively, and gradually changed from a blunt peak to a sharp peak, indicating that the C-O bond on polysaccharides interacted with As and that the content of functional groups increased. The characteristic C-O peak of carboxylic acid shifted from 1,418.91 cm^{-1} to 1,414.00 cm^{-1}, indicating that -COOH played an important role in the adsorption removal of As (Lian et al., 2022; Wei et al., 2017a, 2019b).

In summary, it can be seen from the infrared spectra that EPS is composed of polysaccharides, proteins,

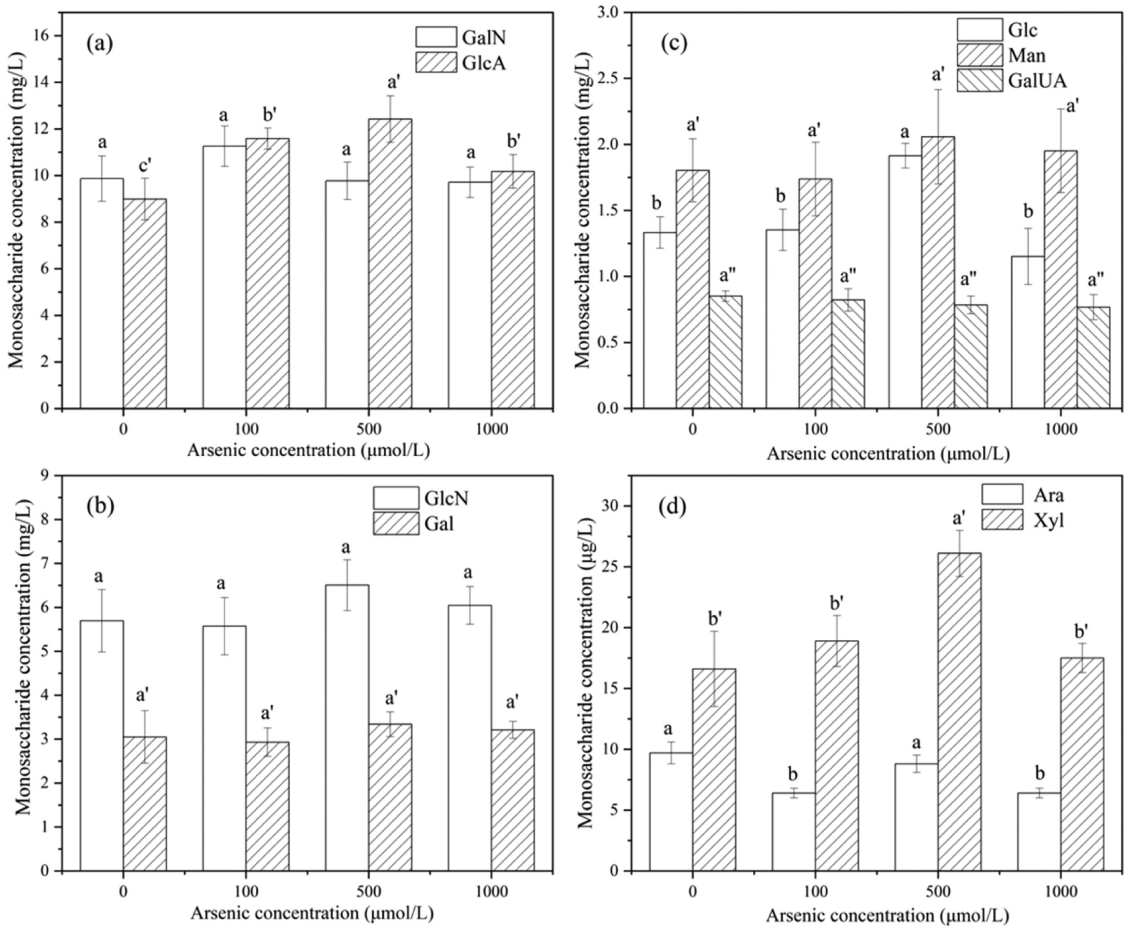

Fig. 3 – Monosaccharide composition in EPS of *Ochrobactrum* sp. cultured at different arsenic concentrations.
Notes: GalN: Galactosamine hydrochloride; GlcA: Glucuronic acid; Glc: Glucose; Man: Mannose; GalUA: Galacturonic acid; GlcN: Glucosamine hydrochloride; Gal: Galactose; Ara: Arabinose; Xyl: Xylose.

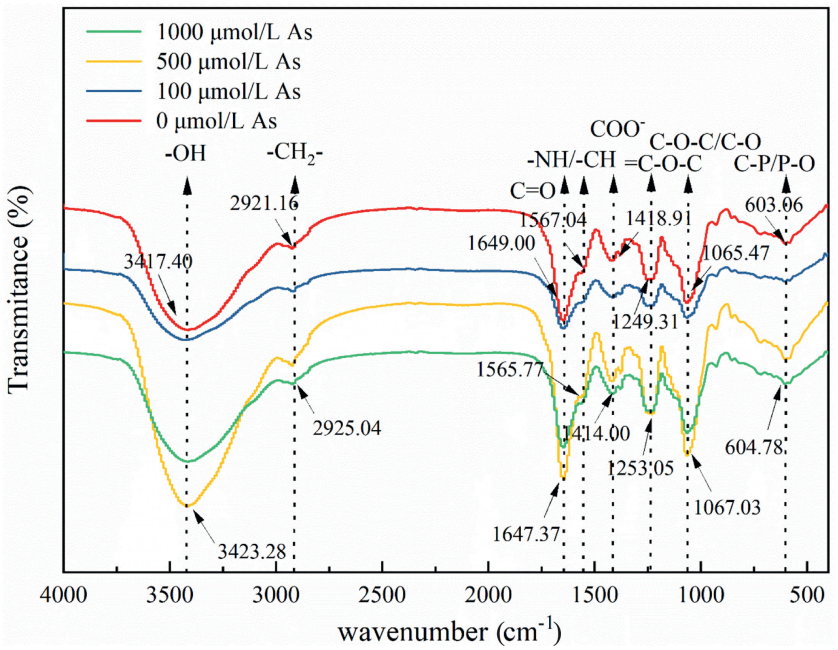

Fig. 4 – FTIR analysis of EPS at different arsenic concentrations.

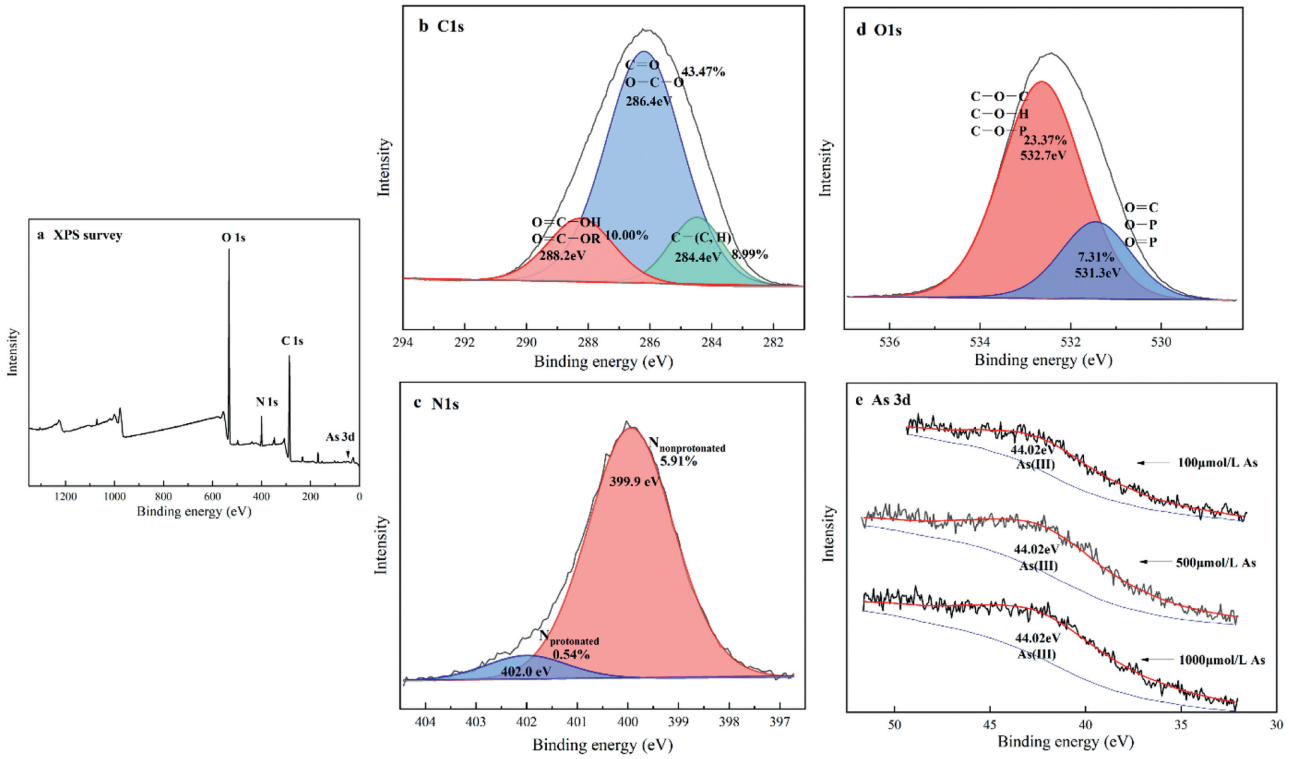

Fig. 5 – XPS analysis of EPS produced at different As concentrations (a: XPS survey; b: C 1s; c: N 1s; d: O 1s; e: As 3d)

and a minuscule amount of nucleic acids. The functional groups of polysaccharides and proteins can bind to As, which is the active component in the adsorption of As by EPS. In addition, -COOH,-OH,-NH,-C=O, and -C-O played an important role in the adsorption of As, consistent with other reports in the literature (Wei et al., 2019; Irshad et al., 2019).

XPS analysis was conducted after the extraction and purification of EPS produced by iron-oxidizing bacteria. **Fig. 5** shows the XPS full spectrum (a), element C (b), N (c), O (d) of EPS from iron-oxidizing bacteria treated with 1,000 μmol/L As, and the XPS peaks of As (e) under different treatments. As shown in **Fig. 5**, the core horizontal peaks were C 1s (286.1 eV), N1 s (400.0 eV), O 1s (532.4 eV), and As 3d (43.83 eV). The mass fractions of C, O, N and P were estimated to be 62.46%, 6.45%, 30.68%, and 0.41%, respectively. Deconvolution was performed on high-resolution scanning of C 1s, O 1s, and N 1s to obtain corresponding functional groups. **Fig. 5** clearly shows three peaks of C (1s), two peaks of O (1s), and two peaks of N (1s). The C 1s peak was split into three peaks: the 288.2 eV peak indicated O=C-OH groups from carboxyl or ester moieties; the peak at 286.4 eV was C=O or O-C-O, which indicates carboxylate, carbonyl, amide, acetal, or semi-acetal groups, which accounted for the largest proportion (43.47%). The peak at 284.4 eV was related to C-(C,H) groups of lipid or amino acid side chains, and the relative proportion was low (8.99%). The N 1s peak was also decomposed into two peaks. The peak at 399.9 eV was attributed to the nonprotonated nitrogen from amines and amides (5.91%), and the other peak at 402.0 eV was attributed to the protonated amine (0.54%), which usually exists in amino acids and amino sugars. The O 1s peak at 532.7 eV (23.37%) was attributed to alcohols, semi-aldols or acetal groups; the O 1s peak at 531.3 eV (7.31%) was formed by C=O groups, such as carboxylates, carbonyls, esters, or amides (Omoike et al., 2004; Yuan et al., 2011). The binding energy of As after adsorption was distributed in the range of 33.13–53.03 eV, and the strongest binding peak was in the range of 43.74–43.83 eV. According to the binding analysis of the XPS database, it was shown that the binding of As was associated with EPS in the form of As^{3+}. **Fig. 5**e shows that the proportion of As^{3+} adsorbed on EPS increased with increasing As concentration.

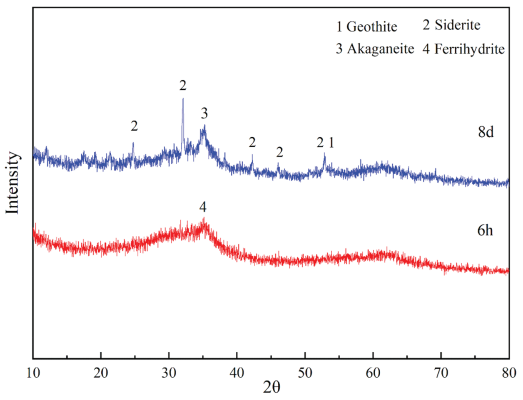

Fig. 6 – XRD patterns of mineral precipitates at different biomineralization time (6 hr and day 8), respectively.

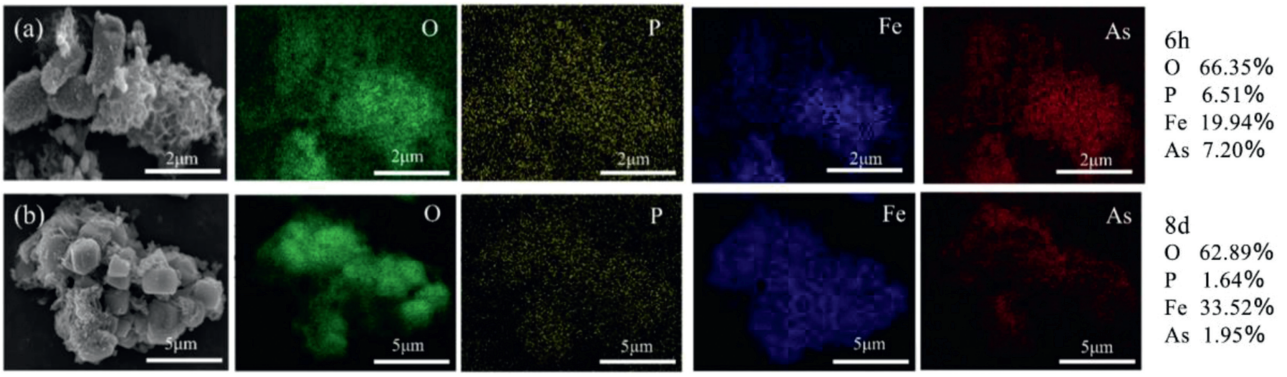

Fig. 7 – Elemental distribution of mineral precipitates in different biomineralization periods (a: 6 hr, b: day 8).

2.4. *Mineralogical changes and surface element analysis of iron-oxidizing bacterial mineralization*

In the above study, we found that a 500 μmol/L arsenic concentration promoted extracellular polymeric substances produced by iron-oxidizing bacteria. We expanded our study to further explore the effects of the same arsenic concentration on the regulation of biomineralization by iron-oxidizing bacteria. At first, SEM-EDS was used to characterize the element distribution on the surface of bacterial-mineral aggregates at different stages, and the evolution of the mineral crystal phase during the biomineralization of iron-oxidizing bacteria was also analysed by XRD.

As shown in **Fig. 6**, at 6 hr of biomineralization, only diffraction peaks of weak crystalline ferrihydrite could be observed in the XRD patterns. In observing the biomineralization process at day 8, the mineral phase in the system changed. It could be seen from the XRD pattern that there were diffraction peaks of goethite, akaganeite, and siderite in the system. Amorphous ferrihydrite is a common iron oxide produced by iron-oxidizing bacteria, but its structure is not stable (Straub et al., 1998). In the process of biomineralization over time, the products would form goethite or haematite with higher crystallinity and a more stable structure through dissolution and recrystallization (Hansel et al., 2005; Rosso et al., 2010; Qian et al., 2021). Relevant studies have shown that Fe(III) in iron (oxyhydr) oxides and Fe(II) adsorbed on them would recrystallize during electron transfer, and the aggregation of ferrihydrite provided the premise for its transformation. Researchers also confirmed that the products of iron-oxidizing bacteria also included siderite, goethite, and akaganeite (Liu et al., 2012).

Fig. 7 shows the surface distribution of elements O, P, Fe, and As at 6 hr (a) and day 8 (b). Fe and O were the two most important elements in biominerals. In the 6 hr SEM-mapping diagram, the elements O, P, Fe, and As were tightly integrated on the surface of the aggregates. Based on the XRD analysis above, due to the amorphous ferrihydrite ($Fe_5HO_8{\cdot}4H_2O$) generated by the initial oxidation of Fe(II) by iron-oxidizing bacteria, the iron minerals with a large specific surface area had more As adsorption sites. Therefore, the distribution of Fe and As was similar. However, these forms of iron were in a metastable state in the environment and could be easily transformed from the mineral phase and morphological structure under the action of chemistry or microorganisms to form iron minerals with high crystallinity and more stability, such as cilia, haematite, goethite, and magnetite (Lu et al., 2014). This process was often accompanied by the migration and release of heavy metals on mineral surfaces, secondary adsorption and immobilization, and coprecipitation. So, as the day 8 (b) showed, with the extension of mineralization time, the element distribution on the surface of bacteria-mineral aggregates changed obviously. The element distribution of Fe and O on the surface of aggregates at day 8 (b) was different from that at 6 hr (a), which was due to the continuous growth of minerals and the transformation of mineral phases. At this time, the main mineral phase had been transformed into higher crystallinity siderite ($FeCO_3$) or nano-goethite (α-FeOOH), and the distribution of As on the mineral surface was significantly less than that at 6 hr (a). This was also due to the decrease in active adsorption sites in the mineral phase with high crystallinity, and the formation of the secondary mineral phase undergoes a dissolution-recrystallization process, which would cause the dissolution and release of heavy metals adsorbed in the original mineral (Sheals et al., 2002; Islam et al., 2004; Gao et al., 2022). The distribution of As showed that As preferentially adsorbed at the edge of iron minerals, which was consistent with Perez et al., (2020).

3. Conclusion

The extracellular polymeric substances (EPS) secreted by iron-oxidizing bacteria (*Ochrobactrum* EEELCW01) enabled them to tolerate arsenic (As) in a specific concentration range. The main component of EPS secreted by iron-oxidizing bacteria was composed of polysaccharides followed by considerably smaller amounts of proteins; the polysaccharide content was 150.76-165.33 mg/g DW, and the protein content was 12.98-16.12 mg/g DW. Low concentrations of As (100 or 500 μmol/L) promoted the amount of EPS secretion, which was inhibited at high concentrations of As (1000 μmol/L). FTIR results showed that EPS was composed of polysaccharides, proteins, and a miniscule amount of nucleic acids. XPS results showed that As was bound to EPS in the form of As^{3+}. With the increasing As concentration, the proportion of As^{3+} adsorbed on EPS

increased. Ferrihydrite with a weak crystalline state was only produced in the system at 6 hr during the mineralization process of *Ochrobactrum* sp. With the extension of mineralization time, at day 8 , the main mineral phases were transformed from weakly crystalline hydrous iron ore into higher crystallinity siderite ($FeCO_3$) or goethite (α-FeOOH), and the specific surface area and active sites of minerals were reduced, resulting in the dissolution, release, and redistribution of As adsorbed by the original minerals. As/Fe also showed a decreasing trend with the increasing time. It can be seen from the distribution of As elements that As is preferentially adsorbed on the edges of iron minerals. In summary, the results of this study provide further evidence for the potential role of iron-oxidizing bacteria in the As biomineralization and remediation.

Declaration of Competing Interest

The work described was original research that has not been published previously, and not under consideration for publication elsewhere, in whole or in part. No conflict of interest exits in the submission of this manuscript, and manuscript is approved by all authors for publication. All co-authors listed have approved the submission of this manuscript.

Acknowledgment

This work was supported by the National Natural Science Foundation of China (No. 42177392), and the Dean's Research Fund 2020/21 (No. 04626) of the Education University of Hong Kong.

REFERENCE

Adav, S.S., Lee, D.J., 2008. Extraction of extracellular polymeric substances from aerobic granule with compact interior structure. J. Hazard. Mater. 154 (1–3), 1120–1126.

Alka, S., Shahir, S., Ibrahim, N., Ndejiko, M.J., Vo, DV.N., Abd Manan, F., 2020. Arsenic removal technologies and future trends: a mini review. J. Clean. Prod. 278.

Bhunia, B., Uday, U.S.P., Oinam, G., Mondal, A., Bandyopadhyay, T.K., Tiwari, O.N., 2018. Characterization, genetic regulation and production of cyanobacterial xopolysaccharides and its applicability for heavy metal removal. Carbohyd. Polym. 179, 228–243.

Bradford, M.M., 1976. A rapid and sensitive method for the quantitation of microgram quantities of protein utilizing the principle of protein-dye binding. Anal. Biochem. 72, 248–254.

Cao, Y.Y., 2013. Mechanism and Environmental Effects of Bacterial Extracellular Polymers on Soil solid Phase Interface. Huazhong Agricultural University, Wuhan, Hubei Province, China.

Chan, C.S., Fakra, S.C., Edwards, D.C., Emerson, D., Banfield, J.F., 2009. Iron oxyhydroxide mineralization on microbial extracellular polysaccharides. Geochim. Cosmochim. Acta. 73 (13), 3807–3818.

Chan, C.S., De Stasio, G., Welch, S.A., Girasole, M., Frazer, B.H., Nesterova, M.V., et al., 2004. Microbial polysaccharides template assembly of nanocrystal fibres. Science 303 (5664), 1656–1658.

Chen, L.X., Zhang, M., Shi, J.J., Zhang, D., Guo, Y., Bao, Z.H., 2020. Research progress on arsenic tolerance mechanism of iron-oxidizing bacteria and its application in arsenic pollution remediation. Microbiol. China 47 (09), 3054–3064.

Clapa, T., Narozna, D., Siuda, R., Borkowski, A., Selwet, M., Madrzak, C., 2019. Diversity of bacterial communities in the acid mine drainage ecosystem of an abandoned polymetallic mine in Poland. Pol. J. Environ. Stud. 28 (4), 2109–2119.

DuBois, M., Gilles, K.A., Hamilton, J.K., Rebers, P.A., Smith, F., 1956. Colorimetric method for determination of sugars and related substances. Anal. Chem. 28 (3), 350–356.

Gao, M.S., Su, Y., Gao, J.B., Zhong, X.W., Li, H., Wang, H.J., et al., 2022. Arsenic speciation transformation in soils with high geological background: new insights from the governing role of Fe. Chemosphere 302.

Gehrke, Telegdi, Thierry, Sand., 1998. Importance of extracellular polymeric substances from thiobacillus ferrooxidans for bioleaching. Appl. Environ. Microb. 64 (7), 2743–2747.

Govarthanana, M., Kamala-Kannan, S., Selvankumar, T., Mythili, R., Srinivasan, P., Kim, H., 2019. Effect of blue light on growth and exopolysaccharides production in phototrophic *Rhodobacter* sp. BT18 isolated from brackish water. Int. J. Biol. Macromol. 131, 74–80.

Hansel, C.M., Benner, S.G., Fendorf, S., 2005. Competing Fe(II)-induced mineralization pathways of ferrihydrite. Environ. Sci. Technol. 39 (18), 7147–7153.

Hou, W.J., Ma, Z.Q., Sun, L.L., Han, M.S., Lu, J.J., Li, Z.X., et al., 2013. Extracellular polymeric substances from copper-tolerance Sinorhizobium meliloti immobilize Cu^{2+}. J. Hazard. Mater. 261, 614–620.

Huang, F., Zhou, F., Jiang, S.Y., Zhang, J.Y., 2019. Effects of extracellular polymeric substances on the bioaccumulation of inorganic arsenic by green microalgae. Environ. Chem. 38 (5), 1021–1027.

Irshad, S., Xie, Z.M., Jia, W., Nawaz, A., Luo, Y., Wang, Y.X., et al., 2019. Indigenous strain *Bacillus* XZM assisted phytoremediation and detoxification of arsenic in *Vallisneria denseserrulata*. J. Hazard. Mater. 381.

Islam, F.S., Gault, A.G., Boothman, C., Polya, D.A., Charnock, J.M., Chatterjee, D., et al., 2004. Role of metal-reducing bacteria in arsenic release from Bengal delta sediments. Nature 430 (6995), 68–71.

Iwahori, K., Watanabe, J.I., Tani, Y., Seyama, H., Miyata, N., 2014. Removal of heavy metal cations by biogenic magnetite nanoparticles produced in Fe(III)-reducing microbial enrichment cultures. J. Biosci. Bioeng. 117 (3), 333–335.

Kang, F.X., Qu, X.L., Alvarez, P.J., Zhu, D.Q., 2017. Extracellular saccharide-mediated reduction of Au^{3+} to gold nanoparticles: new insights for heavy metals biomineralization on microbial surfaces. Environ. Sci. Technol. 51, 2776–2785.

Kappler, A., Straub, K.L., 2005. Geomicrobiological cycling of iron. Rev. Mineral. Geochem. 59, 85–108.

Katsoyiannis, I.A., Zouboulis, A.I., 2004. Application of biological processes for the removal of arsenic from groundwaters. Water Res 38 (1), 17–26.

Khan, I., Awan, S.A., Rizwan, M., Ali, S., Zhang, X.Q., Huang, L.K., 2021. Arsenic behavior in soil-plant system and its detoxification mechanisms in plants: a review. Environ. Pollut. 286.

Lee, Y.C., 1990. High-performance anion-exchange chromatography for carbohydrate analysis. Anal. Biochem. 189 (2), 151–162.

Li, H.M., Wei, M., Min, W.H., Gao, Y.W., Liu, X.Q., Liu, J.S., 2016. Removal of heavy metal ions in aqueous solution by exopolysaccharides from *Athelia rolfsii*. Biocatal. Agr. Biotech. 6, 28–32.

Lian, Z.Y., Yang, Z.Y., Song, W.F., Sun, M.G., Xiao, Y.G., Bai, Y., 2022. Effects of different exogenous cadmium compounds on the

chemical composition and adsorption properties of two gram-negative bacterial EPS. Sci. Total Environ. 806.
Liu, H., Li, P., Wang, H.L., Qing, C., Tan, T., Shi, B., 2020. Arsenic mobilization affected by extracellular polymeric substances (EPS) of the dissimilatory iron reducing bacteria isolated from high arsenic groundwater. Sci. Total Environ. 735.
Liu, H.Y., Wang, H.H., Cui, C.H., Wang, M., Guo, J.J., Wen, Z.P., et al., 2013. Experiment improvement of the soluble sugar content determination by enthrone colorimetric method. Laboratory Science 16 (02), 19–20.
Liu, Q., 2012. Arsenic Resistance and Arsenic Removal Characteristics of Iron-Oxidizing Bacteria. University of Geosciences, Wuhan, Hubei Province, China.
Lu, X.X., Huangfu, X.L., Ma, J., 2014. Removal of trace mercury(II) from aqueous solution by in situ formed Mn-Fe (hydr)oxides. J. Hazard. Mater. 280, 71–78.
Luo, X.H., Jiang, X.X., Xue, S.G., Tang, X.J., Zhou, C.H., Wu, C., et al., 2020. Arsenic biomineralization by iron oxidizing strain (*Ochrobactrum* sp.) isolated from a paddy soil in Hunan. China. Land Degrad. Dev. 32 (6), 2082–2093.
Miot, J., Benzerara, K., Obst, M., Kappler, A., Hegler, F., Schadler, S., et al., 2009. Extracellular iron biomineralization by photoautotrophic iron-oxidizing bacteria. Appl. Environ. Microb. 75 (17), 5586–5591.
Naveed, S., Yu, Q.N., Zhang, C.H., Ge, Y., 2020. Extracellular polymeric substances alter cell surface properties, toxicity, and accumulation of arsenic in *Synechocystis* PCC6803. Environ. Pollut. 261.
Ngo, H.T.T., Liang, L., Nguyen, D.B., Doan, H.N., Watchalayann, P., 2021. Blood heavy metals and DNA damage among children living in an informal E-waste processing area in Vietnam. Hunan and Ecological Risk Assessment 27 (2), 541–559.
Omoike, A., Chorover, J., 2004. Spectroscopic study of extracellular polymeric substances from Bacillus subtilis: Aqueous chemistry and adsorption effect. Biomacromolecules 5 (4), 1219–1230.
Pan, X., Fu, Q., Zhang, D., 2012. Biomineralization based remediation of As(III) contaminated soil by Sporosarcina ginsengisoli. J. Hazard. Mater. 20, 178–184.
Peng, J.Y., Zhang, S., Han, Y.Y., Bate, B., Ke, H., Chen, Y.M., 2021. Soil heavy metal pollution of industrial legacies in China and health risk assessment. Sci. Total Environ. 816.
Perez, J.P.H, Freeman, H.M., Brown, A.P., van Genuchten, C.M., Dideriksen, K., S'ari, M., et al., 2020. Direct visualization of arsenic binding on green rust sulfate. Environ. Sci. Technol. 54 (6), 3297–3305.
Qian, Z.Y., Wu, C., He, X., Xue, S.G., 2021. Study on the influence of iron redox cycling microorganism on heavy metals in the environment. Environ. Chem. 40 (03), 834–850.
Razzak, A., Shafiquzzaman, Md., Haider, H., Alresheedi, M., 2021. Arsenic removal by iron-oxidizing bacteria in a fixed-bed coconut husk column: Experimental study and numerical modeling. Environ. Pollut. 272.
Rosso, K.M., Yanina, S.V., Gorski, C.A., Larese-Casanova, P., Scherer, M.M., 2010. Connecting observations of hematite (alpha-Fe_2O_3) growth catalyzed by Fe(II). Environ. Sci. Technol. 44 (1), 61–67.
Saba, Rehman, Y., Ahmed, M., Sabri, A.N., 2019. Potential role of bacterial extracellular polymeric substances as biosorbent material for arsenic bioremediation. Bioremediat. J. 23 (2), 72–81.
Sheals, J., Sjoberg, S., Persson, P., 2002. Adsorption of glyphosate on goethite: Molecular characterization of surface complexes. Environ. Sci. Technol. 36 (14), 3090–3095.
Straub, K.L., Hanzlik, M., Buchholz-Cleven, B.E., 1998. The use of biologically produced ferrihydrite for the isolation of novel iron-reducing bacteria. Syst. Appl. Microbiol. 21, 442–449.
Sun, Z.Y., Huang, J.B., 2006. Dextran molecules on the modulation of iron hydroxide mineralization crystallization. J. Phys. Chem. 2, 172–177.
Wei, L.L., Li, J.J., Xue, M., Wang, S., Li, Q.Y., Qin, K.N., et al., 2019. Adsorption behaviors of Cu^{2+}, Zn^{2+} and Cd^{2+} onto proteins, humic acid, and polysaccharides extracted from sludge EPS: sorption properties and mechanisms. Bioresour. Technol. 291.
Wei, L.L., Li, Y., Noguera, D.R., Zhao, N.B., Song, Y., Ding, J., et al., 2017. Adsorption of Cu^{2+} and Zn^{2+} by extracellular polymeric substances (EPS) in different sludges: effect of EPS fractional polarity on binding mechanism. J. Hazard. Mater. 321, 473–483.
Wu, K.K., Wu, C., Jiang, X.X., Xue, R., Pan, W.S., Li, W.C., et al., 2022. Remediation of arsenic-contaminated paddy field by a new iron oxidizing strain (*Ochrobactrum* sp.) and iron-modified biochar. J. Environ. Sci. 115, 411–421.
Xiu, W., Guo, H., Liu, Q., Liu, Z.Y., Zou, Y.E., Zhang, B.G., 2015. Arsenic removal and transformation by *Pseudomonas* sp. strain GE-1-induced ferrihydrite: coco-precipitation versus adsorption. Water Air Soil Poll 226 (6), 167.
Xue, S.G., He, X., Jiang, X.X., Pan, W.S., Li, W., Wu, C., et al., 2022. Arsenic biotransformation genes and As transportation in soil-rice system affected by iron-oxidizing strain (*Ochrobactrum* sp.). Environ. Pollut. 314.
Yuan, S.J., Sun, M., Sheng, G.P., Li, Y., Li, W.W., Yao, R.S., et al., 2011. Identification of key constituents and structure of the extracellular polymeric substances excreted by bacillus megaterium tf10 for their flocculation capacity. Environ. Sci. Technol. 45 (3), 1152–1157.
Zeng, J.Q., Li, C.X., Wang, J.T., Tang, L., Wu, C., Xue, S.G., 2022. Pollution simulation and remediation strategy of a zinc smelting site based on multi-source information. J. Hazard. Mater. 433.
Zhang, L.K., Qin, X.Q., Tang, J.S., Liu, W., Yang, H., 2017. Review of arsenic geochemical characteristics and its significance on arsenic pollution studies in karst groundwater. Southwest China. Appl. Geochem. 77, 80–88.
Zhang, J.Y., Zhou, F., Liu, Y.X., Huang, F., Zhang, C.L., 2020. Effect of extracellular polymeric substances on arsenic accumulation in *Chlorella pyrenoidosa*. Sci. Total Environ. 704.
Zhang, P., Chen, Y.P., Guo, J.S., Shen, Y., Yang, J.X., Fang, F., et al., 2014. Adsorption behavior of tightly bound extracellular polymeric substances on model organic surfaces under different pH and cations with surface plasmon resonance. Water Res 57, 31–39.
Zhou, X.W., 2020. Role of microbial extracellular electron transfer mediated by extracellular polymeric substances in the reduction of typical pollutants. Nanjing University, Nanjing, Jiangsu Province, China.